Article

Why Do the Heavy-Atom Analogues of Acetylene EH (E = Si–Pb) Exhibit Unusual Structures?

Matthias Lein, Andreas Krapp, and Gernot Frenking

J. Am. Chem. Soc., **2005**, 127 (17), 6290-6299• DOI: 10.1021/ja042295c • Publication Date (Web): 07 April 2005

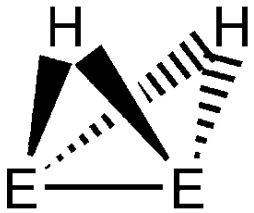

A

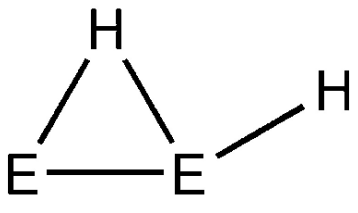

B

More About This Article

Additional resources and features associated with this article are available within the HTML version:

- Supporting Information
- Links to the 14 articles that cite this article, as of the time of this article download
- Access to high resolution figures
- Links to articles and content related to this article
- Copyright permission to reproduce figures and/or text from this article

View the Full Text HTML

J|A|C|S
ARTICLES
Published on Web 04/07/2005

Why Do the Heavy-Atom Analogues of Acetylene E_2H_2 (E = Si−Pb) Exhibit Unusual Structures?

Matthias Lein,[†,§] Andreas Krapp,[†] and Gernot Frenking*[,†]

Contribution from the Fachbereich Chemie, Philipps-Universität Marburg, Hans-Meerwein-Strasse, D-35032 Marburg, Germany, and the Theoretical and Computational Chemistry Research Centre, Institute of Fundamental Sciences, Massey University, Albany Campus, Bldg. 44, Private Bag 102904 North Shore MSC, Auckland, New Zealand

Received December 22, 2004; E-mail: frenking@chemie.uni-marburg.de

Abstract: DFT calculations at BP86/QZ4P have been carried out for different structures of E_2H_2 (E = C, Si, Ge, Sn, Pb) with the goal to explain the unusual equilibrium geometries of the heavier group 14 homologues where E = Si−Pb. The global energy minima of the latter molecules have a nonplanar doubly bridged structure **A** followed by the singly bridged planar form **B**, the vinylidene-type structure **C**, and the trans-bent isomer **D1**. The energetically high-lying trans-bent structure **D2** possessing an electron sextet at E and the linear form HE≡EH, which are not minima on the PES, have also been studied. The unusual structures of E_2H_2 (E = Si−Pb) are explained with the interactions between the EH moieties in the ($X^2\Pi$) electronic ground state which differ from C_2H_2, which is bound through interactions between CH in the $a^4\Sigma^-$ excited state. Bonding between two ($X^2\Pi$) fragments of the heavier EH hydrides is favored over the bonding in the $a^4\Sigma^-$ excited state because the $X^2\Pi \rightarrow a^4\Sigma^-$ excitation energy of EH (E = Si−Pb) is significantly higher than for CH. The doubly bridged structure **A** of E_2H_2 has three bonding orbital contributions: one σ bond and two E−H donor−acceptor bonds. The singly bridged isomer **B** also has three bonding orbital contributions: one π bond, one E−H donor−acceptor bond, and one lone-pair donor−acceptor bond. The trans-bent form **D1** has one π bond and two lone-pair donor−acceptor bonds, while **D2** has only one σ bond. The strength of the stabilizing orbital contributions has been estimated with an energy decomposition analysis, which also gives the bonding contributions of the quasi-classical electrostatic interactions.

1. Introduction

The history of chemical research in the field of heavy-atom group 14 analogues of acetylene E_2H_2 and its substituted derivatives E_2R_2 (E = Si−Pb) that was carried out in the last 20 years is a fascinating chapter of modern chemistry.[1] At the same time it is a beautiful example how theoretical and experimental methods fruitfully complement and challenge each other. Experimental attempts to isolate molecules that possess a triple bond E≡E with E = Si−Pb were not successful for a long time. The starting signal for positive results came from theory. In 1983 Lischka and Köhler[2] reported on quantum chemical calculations that showed that the singlet potential energy surface (PES) of Si_2H_2 is very different from that of C_2H_2. The acetylene-like linear species HSi≡SiH was found not to be an energy minimum structure. Structure **E** (Scheme 1) has two imaginary frequencies, which means that it is a second-order saddle point on the PES. Note that the bonding lines that are drawn in Scheme 1 indicate only the atomic connectivities but not the degree or nature of the bonding.

Scheme 1

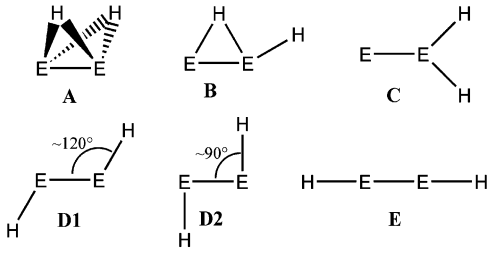

The energetically lowest lying form of Si_2H_2 was predicted to be the doubly hydrogen-bridged butterfly structure **A** (Scheme 1).[2] Geometry optimization of **E** without linearity constraint yields the trans-bent structure **D1** as a higher lying energy minimum form. The vinylidene isomer **C** was calculated to be another minimum on the PES that is lower in energy than **D1** but higher lying than **A**. The calculations also showed that triplet structures of Si_2H_2 are higher in energy than the singlet forms.[2] Subsequent theoretical studies on Si_2H_2 isomers confirmed the results of Lischka and Köhler,[2] but the isomer **B** was found as yet another low-lying energy minimum.[3] Later calculations on Ge_2H_2,[4,5] Sn_2H_2,[5] and Pb_2H_2[5,6,10] showed that the energy minimum structures and their relative energies are similar to the calculated results of Si_2H_2.

[†] Philipps-Universität Marburg.
[§] Massey University.

(1) Recent reviews: (a) Weidenbruch, M. *Angew. Chem.* **2003**, *115*, 2322. *Angew. Chem., Int. Ed.* **2003**, *42*, 2222. (b) Weidenbruch, M. *J. Organomet. Chem.* **2002**, *646*, 39. (c) Power, P. P. *Chem. Rev.* **1999**, *99*, 3463.
(2) Lischka, H.; Köhler, H. *J. Am. Chem. Soc.* **1983**, *105*, 6646.

10.1021/ja042295c CCC: $30.25

The theoretical predictions[2,3] about the unusual structures **A** and **B** were confirmed by spectroscopic studies on Si_2H_2 in low-temperature matrixes by Bogey et al.[7] Hydrogen-bridged structures have recently been identified in low-temperature matrixes also for Ge_2H_2, Sn_2H_2, and Pb_2H_2 besides Si_2H_2 by Andrews and co-workers.[8] A major breakthrough in the experimental research in the field was made in 2000, when Power et al.[9] reported on the synthesis and X-ray structure analysis of the substituted lead compound R*PbPbR* where R* is a bulky terphenyl substituent (R* = C_6H_3-2,6-$Trip_2$; Trip = C_6H_2-2,4,6-*i*Pr_3; Pr = propyl). A peculiar aspect of the molecular structure is the acute C−Pb−Pb bond angle of 94.3° and the rather long Pb−Pb distance of 3.188 Å.[9] The authors suggested that the compound R*PbPbR* has a Pb−Pb single bond where each lead atom carries a σ electron lone-pair. A following theoretical study by Frenking et al.[10] showed that Power's compound R*PbPbR* is a derivative of the Pb_2H_2 isomer **D2** (Scheme 1) that was not considered before. The analysis of the electronic structures of the **D1** and **D2** forms of Pb_2H_2 revealed that the HOMO and the LUMO of the two species are exchanged. The former species has an occupied Pb−Pb π orbital as HOMO, which is unoccupied in the latter form. The HOMO of **D2** is a nonbonding σ lone-pair type orbital. Thus, the lead atoms in **D2** and in R*PbPbR* have an electron sextet in the valence shell, which is not uncommon for lead compounds.[11]

Shortly after Power reported on the synthesis of R*PbPbR* the same author succeeded in the isolation and X-ray structure analysis of the lighter group 14 compounds R′SnSnR′[12] and R′GeGeR′[13] where R′ is a slightly modified terphenyl substituent (R′ = C_6H_3-2,6-$Dipp_2$; Dipp = C_6H_3-2,6-*i*Pr_2). Unlike the lead compound R*PbPbR*, the geometries of the latter tin and germanium analogues of alkynes have bond angles C−E−E that are between 125° and 128°, and they have rather short E−E distances, which indicate a multiple bond.[12,13] This indicates that R′SnSnR′ and R′GeGeR′ are probably derivatives of structure type **D1** but not **D2** (Scheme 1). A related diaryl compound of silicon could not be synthesized until now. The synthesis of the molecule $(R_2MeSi)SiSi(SiMeR_2)$ with R = *t*Bu_3-Si has been reported by Wiberg et al.[14] The compound could not be characterized by X-ray structure analysis, but the ^{29}Si NMR chemical shift was interpreted in favor of a structure where the central silicon atoms are disubstituted. A definite proof for the synthesis of a disilyne was recently given by Sekiguchi et al.,[15] who reported on the X-ray structure analysis of (R_2*i*Pr Si)SiSi(Si*i*PrR_2) where R = $CH(Me_3Si)_2$.

The assignment of the observed ^{29}Si NMR signal to a silicon compound having the structure **D1** by Wiberg et al.[14] was supported by quantum chemical calculations of Nagase, who calculated the structure and the theoretical NMR spectrum of $(R_2MeSi)SiSi(SiMeR_2)$.[16a] Nagase and co-workers made important contributions to the understanding of stable group 14 compounds REER where R is a very bulky substituent.[5,16] They optimized not only the model compounds HEEH but also the structures that were experimentally found by Power[12,13] and Wiberg,[14] and they analyzed the influence of the substituent on the stability of the molecules.

There has been much debate about the bonding situation of the trans-bent structures REER which are derived from **D1** or **D2** (Scheme 1).[1,5,10,16,17] The main topic of the debate was the question why compounds that are substituted analogues of **D1** prefer to have a trans-bent distorted geometry and not a linear structure like acetylenes. Another hotly debated topic was the question whether molecules with the structures **D1** have a E−E triple bond or not. However, a pivotal question that was not addressed in the discussion concerns the explanation of the unusual structures **A**−**D** of the parent compounds E_2H_2. Structures **D1** and **D2** are those that look most similar to linear acetylene, but they are the highest lying forms of E_2H_2 shown in Scheme 1. The preference of molecules REER where R is a heavier group 14 element than carbon has been explained by Popelier et al.[17c] using a topological analysis of the electron density, by Shaik et al.,[17a] who employed VB structures, and by Nagase et al.,[5,16b] who used a MO model that was introduced earlier by Trinquier and Malrieu[18a] and by Carter and Goddard.[18b] However, none of the studies discussed the question why the most stable structures of Si_2H_2−Pb_2H_2 are the doubly bridged form **A** followed by the singly bridged **B**, which is similar in energy to the vinylidene form **C**.

In this work we present a bonding analysis of the E−E bonds in the structures **A**, **B**, **D1**, **D2**, and **E** of Si_2H_2−Pb_2H_2. It will be shown that the unusual hydrogen-bridged forms **A** and **B**

(3) (a) Binkley, J. S. *J. Am. Chem. Soc*. **1984**, *106*, 603. (b) Kalcher, J.; Sax, A.; Olbrich, G. *Int. J. Quantum Chem*. **1984,** *25*, 543. (c) Köhler, H.-J.; Lischka, H. *Chem. Phys. Lett*. **1984**, *112*, 33. (d) Clabo, D. A.; Schaefer, H. F. *J. Chem. Phys*. **1986**, *84*, 1664. (e) Thies, B. S.; Grev, R. S.; Schaefer, H. F. *Chem. Phys. Lett*. **1987**, *140*, 355. (f) Koseki, S.; Gordon, M. S. *J. Phys. Chem*. **1988**, *92*, 364. (g) Koseki, S.; Gordon, M. S. *J. Phys. Chem*. **1989**, *93*, 118. (h) Colegrove, B. T.; Schaefer, H. F. *J. Phys. Chem*. **1990**, *94*, 5593. (i) Colegrove, B. T.; Schaefer, H. F. *J. Am. Chem. Soc*. **1991**, *113*, 1557. (j) Grev, R. S.; Schaefer, H. F. *J. Chem. Phys*. **1992**, *97*, 7990.

(4) (a) Grev, R. S.; De Leeuw, B. J.; Schaefer, H. F. *Chem. Phys. Lett*. **1990**, *165*, 257. (b) Grev, R. S. *Adv. Organomet. Chem*. **1991**, *33*, 125. (c) Palagyi, Z.; Schaefer, H. F.; Kapuy, E. *J. Am. Chem. Soc*. **1993**, *115*, 6901. (d) Li, Q.-S.; Lü, R.-H.; Xie, Y.; Schaefer, H. F. *J. Comput. Chem*. **2002**, *23*, 1642.

(5) Nagase, S.; Kobayashi, K.; Takagi, N. *J. Organomet. Chem*. **2000**, *611*, 264.

(6) Han, Y.-K.; Bae, C.; Lee, Y. S.; Lee, S. Y. *J. Comput. Chem.* **1998**, *19*, 1526.

(7) (a) Bogey, M.; Bolvin, H.; Demuyneck, C.; Destombes, J.-L. *Phys. Rev. Lett*. **1991**, *66*, 413. (b) Cordonnier, M.; Bogey, M.; Demuynck, C.; Destombes, J.-L. *J. Chem. Phys*. **1992**, *97*, 7984. For a review see: Karni, M.; Apeloig, Y.; Kapp, J.; Schleyer, P. v. R. In *The Chemistry of Organic Silicon Compounds*; Apeloig, Y., Ed.; Wiley: Chichester, 2001; Vol. 3, p 1.

(8) (a) Wang, X.; Andrews, L.; Kushto, G. *J. Phys. Chem. A* **2002**, *106*, 5809. (b) Wang, X.; Andrews, L.; Chertihin, G. V.; Souer, P. F. *J. Phys. Chem. A* **2002**, *106*, 6302. (c) Andrews, L.; Wang, X. *J. Phys. Chem. A* **2002**, *106*, 7697. (d) Wang, X.; Andrews, L. *J. Am. Chem. Soc*. **2003**, *125*, 6581.

(9) Pu, L.; Twamley, B.; Power, P. P. *J. Am. Chem. Soc.* **2000**, *122*, 3524.

(10) Chen, Y.; Hartmann, M.; Diedenhofen, M.; Frenking, G. *Angew. Chem., Int. Ed*. **2001**, *40*, 2052.

(11) For a theoretical study of the stability of lead compounds with electron sextet at Pb see: Kaupp, M.; Schleyer, P. v. R. *J. Am. Chem. Soc*. **1993**, *115*, 1061.

(12) Phillips, A. D.; Wright, R. J.; Olmstead, M. M.; Power, P. P. *J. Am. Chem. Soc.* **2002**, *124*, 5930.

(13) Stender, M.; Phillips, A. D.; Wright, R. J.; Power, P. P. *Angew. Chem.* **2002**, *114*, 1863. *Angew. Chem., Int. Ed.* **2002**, *41*, 1785.

(14) (a) Wiberg, N.; Niedermeyer, Fischer, G.; Nöth, H.; Suter, M. *Eur. J. Inorg. Chem*. **2002**, 1066. (b) Wiberg, N.; Vasisht, S. K.; Fischer, G.; Mayer, P. *Z. Allg. Anorg. Chem.* **2004**, *630*, 1823.

(15) Sekiguchi, A.; Kinjo, R.; Ichinohe, M. *Science* **2004**, *305*, 1755.

(16) (a) Takagi, N.; Nagase, S. *Eur. J. Inorg. Chem*. **2002**, 2775. (b) Kobayashi, K.; Nagase, S. *Organometallics* **1997**, *16*, 2489. (c) Kobayashi, K.; Takagi, N.; Nagase, S. *Chem. Lett.* **2001**, 966. (d) Kobayashi, K.; Takagi, N.; Nagase, S. *Organometallics* **2001**, *20*, 234. (e) Takagi, N.; Nagase, S. *Organometallics* **2001**, *20*, 5498.

(17) (a) Danovich, D.; Ogliaro, F.; Karni, M.; Apeloig, Y.; Cooper, D. L.; Shaik, S. *Angew. Chem.* **2001**, *113*, 4146. (b) Grunenberg, J. *Angew. Chem.* **2001**, *113*, 4150. (c) Malcolm, N. O. J.; Gillespie, R. J.; Popelier, P. L. A. *J. Chem. Soc., Dalton Trans*. **2002**, 3333. (d) Himmel, H.-J.; Schnöckel, H. *Chem. Eur. J*. **2003**, *9*, 748.

(18) (a) Trinquier, G.; Malrieu, J.-P. *J. Am. Chem. Soc*. **1987**, *109*, 5303. (b) Trinquier, G.; Malrieu, J.-P. *J. Am. Chem. Soc*. **1989**, *111*, 5916. (c) Carter, E. A.; Goddard, W. A. *J. Phys. Chem.* **1986**, *90*, 998. (d) For a discussion of the bonding model see: Driess, M.; Grützmacher, H. *Angew. Chem.* **1996**, *108*, 900. *Angew. Chem., Int. Ed.* **1996**, *35*, 828.

and their higher stability than the other isomers can be explained in terms of HE−EH interactions using molecular orbital arguments. The vinylidene form **C** has not been considered because the connectivity $E-EH_2$ is different from the other isomers. The qualitative bonding model is supported and complemented by a quantitative energy decomposition analysis of the binding interactions. This is the first theoretical work that explains why the lowest lying isomers of $Si_2H_2-Pb_2H_2$ have a doubly bridged geometry and why the next low-lying form has a singly bridged geometry.

2. Methods

The geometries of the molecules have been optimized at the nonlocal DFT level of theory using the exchange functional of Becke[19] in conjunction with the correlation functional of Perdew[20] (BP86). Uncontracted Slater-type orbitals (STOs) were employed as basis functions for the SCF calculations.[21] The basis sets have quadruple-ζ quality augmented by four sets of polarization functions, i.e., two p and two d functions on hydrogen and two d and two f functions on the other atoms. This level of theory is denoted BP86/QZ4P. An auxiliary set of s, p, d, f, g, and h STOs was used to fit the molecular densities and to represent the Coulomb and exchange potentials accurately in each SCF cycle.[22] Scalar relativistic effects have been considered using the zero-order regular approximation (ZORA).[23] The nature of the stationary points on the potential energy surface was characterized by calculating the Hessian matrixes. The calculations were carried out with the program package ADF 2003.[24]

The HE−EH interactions were analyzed by means of the energy partitioning scheme of ADF,[25] which was originally developed independently by Morokuma[26] and by Ziegler and Rauk.[27] The focus of the bonding analysis is the instantaneous interaction energy, ΔE_{int}, of the bond, which is the energy difference between the molecule and the fragments in the electronic reference state and frozen geometry of the compound. The electronic reference state of EH in structures **A**, **B**, **D1**, and **D2** is $^2\Pi$, while the reference state for **E** is $^4\Sigma^-$. The interaction energy can be divided into three main components:

$$\Delta E_{int} = \Delta E_{elstat} + \Delta E_{Pauli} + \Delta E_{orb} \quad (1)$$

ΔE_{elstat} gives the electrostatic interaction energy between the fragments, which are calculated using the frozen electron density distribution of the fragments EH in the geometry of the molecules E_2H_2. The second term in eq 1, ΔE_{Pauli}, refers to the repulsive interactions between the fragments, which are caused by the fact that two electrons with the same spin cannot occupy the same region in space. ΔE_{Pauli} is calculated by enforcing the Kohn−Sham determinant on the superimposed fragments to obey the Pauli principle by antisymmetrization and renormalization. The stabilizing orbital interaction term, ΔE_{orb}, is calculated in the final step of the energy partitioning analysis when the Kohn−Sham orbitals relax to their optimal form. This term can be further partitioned into contributions by the orbitals belonging to different irreducible representations of the point group of the interacting system. The interaction energy, ΔE_{int}, can be used to calculate the bond dissociation energy, D_e, by adding ΔE_{prep}, which is the energy necessary to promote the fragments from their equilibrium geometry to the geometry in the compounds (eq 2). Further details of the energy partitioning analysis can be found in the literature.[25b]

$$-D_e = \Delta E_{prep} + \Delta E_{int} \quad (2)$$

The relative energies of the Si_2H_2 stationary points on the lowest lying singlet and triplet PES that were optimized at BP86/QZ4P have also been calculated at the MRCI level using Dunnings correlation-consistent pVQZ basis set, which was augmented by diffuse functions.[28] A full valence reference space with all single and double excitations has been considered in the MRCI-SD/aug-cc-pVQZ calculations. The program package MOLPRO 2000 was used for the latter calculations.[29] The Laplacian distribution of **B** of Si_2H_2 was calculated at BP86/aug-cc-pVQZ//BP86/QZ4P using the program AIMPAC.[30]

3. Geometries and Orbital Analysis

Figure 1 shows the optimized geometries of structures **A**−**E** of E_2H_2 and the relative energies of the isomers with respect to the global energy minimum **A** calculated at the BP86/QZ4P level. The geometries and relative energies are in agreement with previous theoretical calculations at DFT and ab initio levels.[3−6,10,16] We want to point out that only structures **A**, **B**, **C**, and **D1** are predicted as minima on the PES, while **D2** is a transition state. It has been shown before that the bulky substituents in R*PbPbR* are the reason that structure type **D2** becomes an energy minimum.[10] Note that the relative energies of all isomers E_2H_2 increase with respect to **A** when atom E becomes heavier *except for* **D2**. This is because the electron lone-pair at E in **D2** becomes stabilized relative to a bonding electron pair in the other isomers, which eventually leads to the situation where **D2**(Pb_2H_2) becomes lower in energy than **D1**(Pb_2H_2).

The starting point for the bonding analysis of **A**, **B**, **D1**, **D2**, and **E** of $Si_2H_2-Pb_2H_2$ is the diatomic species EH; that is, we consider the molecules as products of the interactions between two EH fragments. We will first qualitatively analyze the orbital interactions between the diatomic species. Our approach is similar to the Trinquier/Malrieu/Carter/Goddard model.[18] Figure 2 shows schematically the electronic ground state ($X^2\Pi$) and the first excited state ($a^4\Sigma^-$) of EH. The calculated and experimental excitation energies $X^2\Pi \rightarrow a^4\Sigma^-$ are also given. The theoretical values at BP86/QZ4P are in excellent agreement with previous data that have been obtained from experimental studies or from previous high-level theoretical calculations.[31] The largest deviation between theory and experiment is found for SiH (2.2 kcal/mol).

(19) Becke, A. D. *Phys. Rev. A* **1988**, *38*, 3098.
(20) Perdew, J. P. *Phys. Rev. B* **1986**, *33*, 8822.
(21) Snijders, J. G.; Baerends, E. J.; Vernooijs, P. *At. Nucl. Data Tables* **1982**, *26*, 483.
(22) Krijn, J.; Baerends, E. J. *Fit Functions in the HFS-Method*, Internal Report (in Dutch); Vrije Universiteit Amsterdam: The Netherlands, 1984.
(23) (a) Chang, C.; Pelissier, M.; Durand, Ph. *Phys. Scr.* **1986**, *34*, 394. (b) Heully, J.-L.; Lindgren, I.; Lindroth, E.; Lundquist, S.; Martensson-Pendrill, A.-M. *J. Phys. B* **1986**, *19*, 2799. (c) van Lenthe, E.; Baerends, E. J.; Snijders, J. G. *J. Chem. Phys.* **1993**, *99*, 4597. (d) van Lenthe, E.; Baerends, E. J.; Snijders, J. G. *J. Chem. Phys.* **1996**, *105*, 6505. (e) van Lenthe, E.; van Leeuwen, R., Baerends, E. J.; Snijders, J. G. *Int. J. Quantum Chem.* **1996**, *57*, 281.
(24) Baerends, E. J.; et al. *ADF 2003-01*; Scientific Computing & Modelling NV: Amsterdam, The Netherlands (http://www.scm.com/), 2003.
(25) (a) Bickelhaupt, F. M.; Baerends, E. J. In *Reviews in Computational Chemistry*; Lipkowitz, K. B., Boyd, D. B., Eds.; Wiley-VCH: New York, 2000; Vol. 15, p 1. (b) te Velde, G.; Bickelhaupt, F. M.; Baerends, E. J.; van Gisbergen, S. J. A.; Fonseca Guerra, C.; Snijders, J. G.; Ziegler, T. *J. Comput. Chem.* **2001**, *22*, 931.
(26) Morokuma, K. *J. Chem. Phys.* **1971**, *55*, 1236.
(27) Ziegler, T.; Rauk, A. *Theor. Chim. Acta* **1977**, *46*, 1.
(28) (a) Kendall, R. A.; Dunning, T. H.; Harrison, R. J. *J. Chem. Phys.* **1992**, *96*, 6796. (b) Davidson, E. R. *Chem. Phys. Lett.* **1996**, *220*, 514.
(29) MOLPRO 2000 is a package of ab initio programs written by H. J. Werner et al.
(30) AIMPAC Program Package, R. F. W. Bader research group, McMaster University, Hamilton, Canada.
(31) Experimental values for the excitation energies of CH and GeH have been taken from: Huber, K. P., Herzberg, G. *Molecular Spectra and Molecular Structure IV. Constants of Diatomic Molecules*; Van Nostrand-Reinhold: New York, 1979. The value for SiH has been taken from an estimated full-CI calculation: Lewerenz, M.; Bruna, P. J.; Peyerimhoff, S. D.; Buenker, R. J. *J. Phys. B* **1983**, *16*, 4511. The values for SnH and PbH stem from MRD-CI calculations. SnH: Alekseyev, A. B.; Liebermann, H. P.; Buenker, R. J.; Hirsch, G. *Mol Phys.* **1996**, *88*, 591. PbH: Balasubramanian, K.; Pitzer, K. S. *J. Phys. Chem.* **1984**, *88*, 1146.

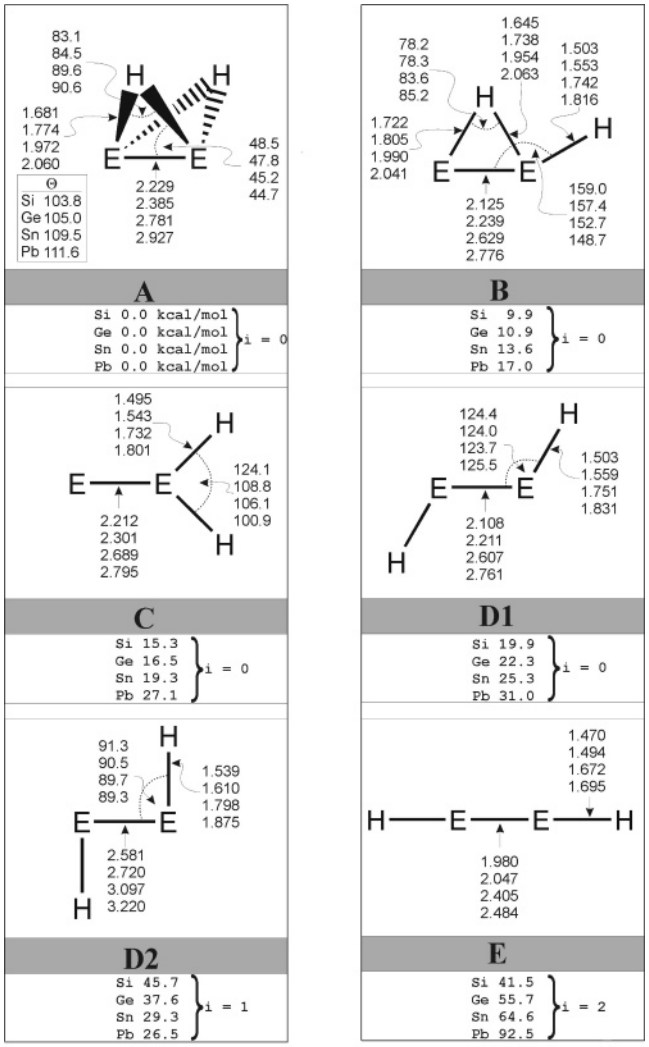

Figure 1. Optimized structures of E_2H_2 isomers **A**−**E** at BP86/QZ4P. Bond lengths are given in Å, angles in deg. The values for Θ give for structure **A** the dihedral angle between the E_2H and E_2H' planes. The relative energies with respect to **A** are given at the bottom of each entry in kcal/mol together with the number of imaginary frequencies i.

The inspection of the electron configurations that are shown in Figure 2 makes it obvious that the electronic reference state of EH in the triply bonded linear species HE≡EH is the $a^4\Sigma^-$ excited state and not the $X^2\Pi$ ground state. The EH fragments must first become excited into the $a^4\Sigma^-$ state in order to bind through a σ and degenerate π bond in HE≡EH (**E**). The electron configuration of the $X^2\Pi$ ground state allows only an electron-sharing single bond between two EH moieties. Figure 2 shows that the carbon species CH has the lowest excitation energy, while the heavier analogues need much more energy to reach the $a^4\Sigma^-$ excited state. This means that it is energetically much easier for CH to excite from the $X^2\Pi$ ground state to the $a^4\Sigma^-$ excited state in order to form a triple bond than for the heavier EH species. The pivotal question that points already toward the reason for the unusual structures of the heavier E_2H_2 addresses the possible gain in binding energy after $X^2\Pi \rightarrow a^4\Sigma^-$ excitation. The answer to the question is given by the data that are listed in Table 1.

The theoretically predicted bond dissociation energies for breaking the triple bond in linear HE≡EH yielding 2 EH ($a^4\Sigma^-$) indicate that acetylene has a very strong bond (Table 1). The

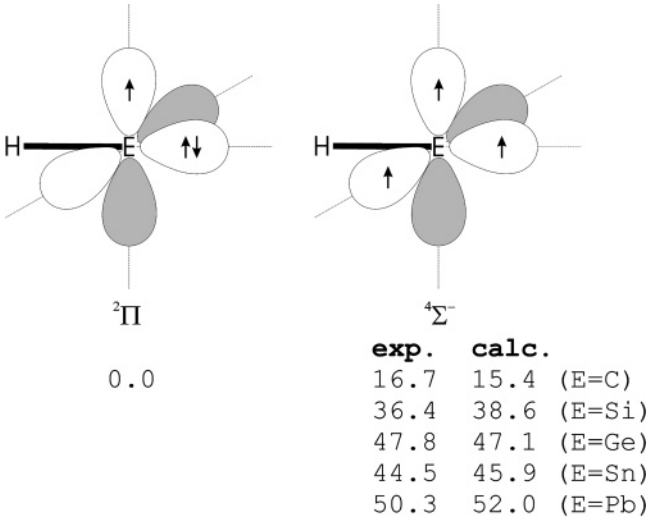

Figure 2. Schematic representation of the electron configuration of the $^2\Pi$ electronic ground state and the $a^4\Sigma^-$ excited state of EH (E = C−Pb). The experimental (ref 31) and calculated (BP86/QZ4P) excitation energies are given in kcal/mol.

Table 1. Calculated Bond Dissociation Energies D_e (kcal/mol) of Linear HE≡EH → 2 EH ($a^4\Sigma^-$) and $X^2\Pi \rightarrow a^4\Sigma^-$ Excitation Energies ΔE_{exc} (kcal/mol) of EH at BP86/QZ4P

E	D_e	ΔE_{exc}	$D_e - 2\Delta E_{exc}$
C	270.9	15.44	240.0
Si	121.6	38.56	44.5
Ge	113.3	47.09	19.0
Sn	89.4	45.87	-2.3
Pb	69.0	52.01	-35.0

calculated value D_e = 270.9 kcal/mol for the above reaction gives after correcting for the excitation energy of the two CH fragments from the $X^2\Pi$ ground state a theoretical bond energy D_e = 240.0 kcal/mol. The inclusion of the zero-point energy contributions yields a bond energy D_o = 231.5 kcal/mol, which is in very good agreement with the experimental value of 228.5 kcal/mol.[32]

The calculated bond dissociation energy D_e = 240.0 kcal/mol for acetylene shows that it is energetically profitable for the CH fragments to form a HC≡CH triple bond through the $a^4\Sigma^-$ excited state because the C−C single bond that can be formed from the $X^2\Pi$ ground state would deliver much less binding energy. Typical C−C single bonds have bond energies of 80−90 kcal/mol.[33] The possibility of additional stabilizations through nonclassical interactions through lone-pair and/or C−H donor acceptor interactions, which are described below, will not be sufficient to match the much higher bond energy of the triple bond.

The situation is very different for the heavier homologues SiH−PbH. The calculations predict that the hypothetical linear molecule HSi≡SiH would have a bond dissociation energy HSi≡SiH → 2 SiH ($a^4\Sigma^-$) of D_e = 121.6 kcal/mol, which is much less than for acetylene. The $X^2\Pi \rightarrow a^4\Sigma^-$ excitation energy for the SiH fragments is $2\Delta E_{exc}$ = 77.1 kcal/mol, which is much higher than for CH (Table 1). Thus, the gain in the binding energy of the silicon system is only $D_e - 2\Delta E_{exc}$ = 44.5 kcal/mol. This is much less than the stabilization energy that can be expected from the formation of an electron-sharing HSi−SiH

(32) Lias, S. G.; Bartmess, J. E.; Liebman, J. F.; Holmes, J. L.; Levin, R. D.; Mallard, W. G. *J. Phys. Chem. Ref. Data* **1988**, *17*, Suppl. 1.

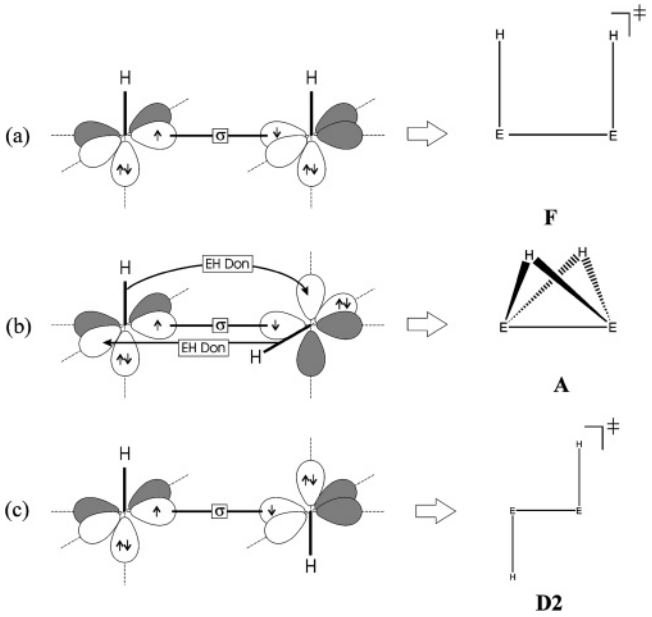

Figure 3. Qualitative model for the orbital interactions between two EH molecules in different orientations where the unpaired electrons yield a σ bond.

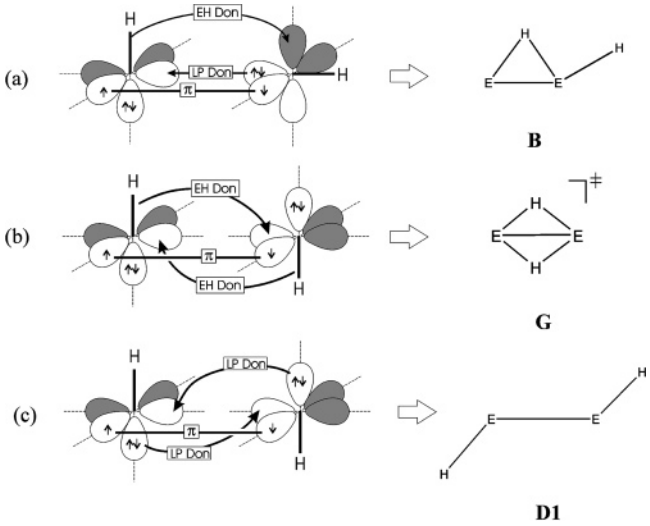

Figure 4. Qualitative model for the orbital interactions between two EH molecules in different orientations where the unpaired electrons yield a π bond.

single bond between SiH in the $X^2\Pi$ ground state. Typical bond dissociation energies of Si−Si single bonds are 75−80 kcal/mol.[33] It follows that it is energetically more profitable for two SiH species to bind in their $X^2\Pi$ ground state than in the $a^4\Sigma^-$ excited state. The same holds true for the heavier homologues GeH−PbH. Table 1 shows that the additional binding energy of the latter diatomics in the linear structure HE≡EH is only 19.0 kcal/mol for E = Ge, which is much less than the binding energy of a typical Ge−Ge single bond. For the tin and lead systems the excitation energies of two EH fragments are even higher than the bond dissociation energy of linear HE≡EH.

The above makes it clear that the bond formation between two EH molecules takes place through the $X^2\Pi$ ground state when E = Si−Pb. Figure 2 shows that a linear arrangement of two ($X^2\Pi$) EH fragments is not favorable for bond formation between the unpaired electrons, which must rather take place in a sideways fashion. Figure 3 shows different orientations for two ($X^2\Pi$) EH which leads to a E−E σ bond.

Figure 3a shows a syn-planar arrangement of the EH moieties, which is not favorable because the vacant p(π) orbitals remain unoccupied while the E−H bonds and the electron lone-pairs of the two molecules repel each other. The geometry optimization of E_2H_2 with a syn-planar arrangement under C_{2v} symmetry constraint gives a structure that has one imaginary frequency; that is, it is a transition state. Rotation about the σ-bond axis by 90° gives a much more favorable arrangement (Figure 3b). Now the empty p(π) orbitals of EH can interact in E_2H_2 with the E−H bond and with the electron lone-pair of the other EH. The stabilization that comes from the donor−acceptor interactions E−H→ p(π) is *stronger* than the donation from the electron lone-pairs (lp) → p(π) for heavier elements E because the lone-pair orbitals have mainly s-character *and* because hydrogen is more electronegative that Si−Pb. This means that the E−H bonds are better donors than the lone-pair orbitals. The E−H bonds are then tilted toward the empty p(π) orbitals of the other EH moiety, which leads to the doubly bridged butterfly structure **A** (Figure 3b). This explains why the global energy minimum form **A** has a hydrogen-bridged geometry that is not planar but has a perpendicular arrangement of the two E_2H planes which have a falting angle between 103.8° and 111.6°. We want to point out that there are three bonding components of the orbital interactions in **A**: one σ bond and two (degenerate) E−H donor−acceptor bonds.

Figure 3c shows the anti-planar arrangement of the EH fragments. The only E−E bonding contribution is the σ orbital between the atoms E. The structure **D2** lacks the two EH donor−acceptor interactions of **A**. The former isomer may become lower in energy than the latter if the hydrogen atoms are substituted by bulky groups such as the terphenyl substituent, which was used by Power in the synthesis of the R*PbPbR* compound.[9]

The unpaired electrons in the $X^2\Pi$ ground state of EH may also be paired in an electron-sharing bond of $(EH)_2$, which has π symmetry with respect to the molecular structure. Figure 4 shows different orientations for two ($X^2\Pi$) EH molecules which lead to a E−E π bond. The arrangement that is given in Figure 4a has an electron lone-pair of one EH moiety pointing in the direction of the empty p orbital of the other EH species. This orbital interaction now has σ symmetry with respect to the $(EH)_2$ dimer. Besides the electron-sharing π bond and the lone-pair (lp) donor−acceptor σ bond, further stabilizing orbital interactions are possible in the structure shown in Figure 4a. This comes from the donation of the EH bonding orbital and possibly the electron lone-pair of that EH molecule, which serves as the lp σ-acceptor (bottom EH in Figure 4a) into the empty p orbital of the lp donor EH (top EH in Figure 4a). As noted before, donation from the EH bonding orbital is stronger than from the lp orbital. The former interaction becomes stronger when the EH donor orbital and the empty p orbital of the interacting fragments are tilted toward each other, which leads to structure **B** (Figure 4a). The tilting of the empty p orbital of the acceptor EH moiety (top EH in Figure 4a) means that the terminal hydrogen atom moves toward the bridging hydrogen atom. The syn orientation of the terminal hydrogen atom with respect to

(33) *Handbook of Chemistry and Physics*, 79th ed.; CRC Press: Boca Raton, 1998.

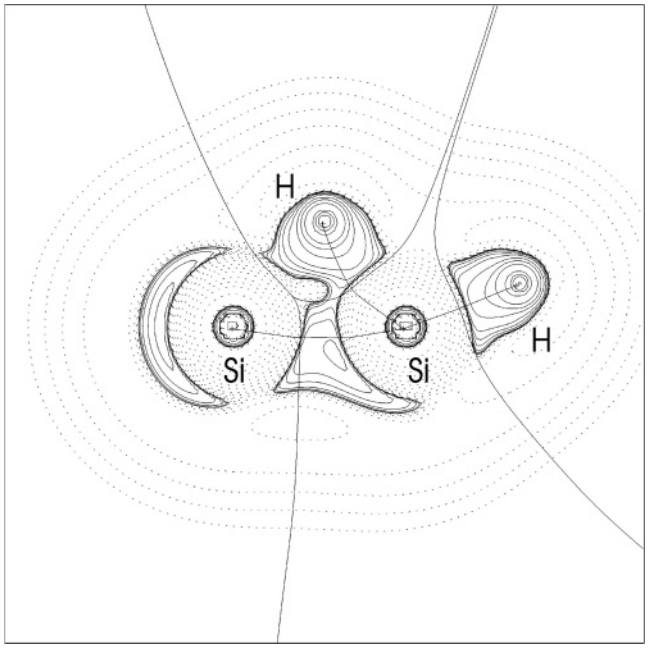

Figure 5. Contour line diagram $\nabla^2\rho(r)$ of isomer **B** of Si_2H_2. Solid lines indicate areas of charge concentration ($\nabla^2\rho(r) < 0$), while dashed lines show areas of charge depletion ($\nabla^2\rho(r) > 0$). Solid lines that connect the atomic nuclei are the bond paths, while solid lines that separate the atomic basins give the zero-flux surfaces in the molecular plane.

the bridging H atom can be explained as a secondary effect of optimizing the EH donor−acceptor interaction, which is shown in Figure 4a. The unusual singly bridged geometry of **B**, which has a terminal hydrogen atom with syn-orientation to the bridging atom, can thus be explained as a stereoelectronic effect that comes from the orbital interactions between EH in the $X^2\Pi$ ground state.

We analyzed the calculated electronic structure of isomer **B** using Si_2H_2 as example in order to see if the electron density distribution is in agreement with the orbital interaction model. Figure 5 shows the Laplacian of the electronic charge distribution $\nabla^2\rho(r)$ in the molecular plane, which is more instructive than the charge distribution $\rho(r)$ because it visually displays relative accumulation of electronic charge. Solid lines indicate areas of charge concentration ($\nabla^2\rho(r) < 0$), while dashed lines show areas of charge depletion ($\nabla^2\rho(r) > 0$). It becomes obvious that there are two areas of charge concentration between the silicon atoms. One area is close to the bridging hydrogen atom, which has a deformed charge distribution with maxima pointing toward both silicon atoms. It is interesting that there is only *one* bond path from the hydrogen atom to one Si atom (right-hand side of Figure 5), while there is no bond path to the other silicon atom. The most important point that supports our orbital interaction model is the area of charge concentration below the Si−Si bond path. This is a visual manifestation of the electron lone-pair donation that is shown in Figure 4a. Note that the maximum of the lone-pair donor−acceptor bond is not on the Si−Si bond path, which indicates that it is a bent bond.

Figure 4b displays another orientation of two EH molecules where the unpaired electrons form a π bond while the EH bonds are in an anti-planar arrangement. The π orbital interaction between the EH fragments is enhanced by two degenerate donor−acceptor interactions between the EH bonding orbitals and the empty p orbitals of the interacting fragments. The latter orbital interactions become stronger when the hydrogen atoms bridge in a doubly bridged planar (D_{2h}) structure. Geometry optimizations of $(EH)_2$ with D_{2h} symmetry constraint show that the optimized form is an energetically low-lying structure on the PES. Inspection of the Hessian matrix reveals, however, that it is a transition state for the degenerate rearrangement of the global energy minimum structure **A**. It is the wing-flapping motion of the butterfly geometry. Structure **A** has a E−E σ bond and two EH donor−acceptor bonds (Figure 3a), while the transition state has a E−E π bond and two EH donor−acceptor bonds (Figure 4b).

The electron lone-pair donation is weaker than the EH donation, but it leads to another structure of $(EH)_2$ which is a minimum on the PES. Figure 4c shows that the lp(EH) → p_π(EH′) donation becomes enhanced by outwardly tilting the E−H bond, which yields the familiar trans form **D1**. The latter species has been synthesized for E = Si, Ge, and Sn with hydrogen being substituted by bulky substituents.[12−15] According to the orbital analysis, structure **D1** has three bonding orbital components, i.e., one π bond and two lp donor−acceptor bonds. Structure **D1** is energetically higher lying than the planar transition state with two bridging hydrogen atoms, which has one π bond and two EH donor−acceptor bonds (right hand side of Figure 4b).[34]

4. Energy Decomposition Analysis

The previous section has shown that the unusual equilibrium geometries **A**−**D2** of E_2H_2 for E = Si−Pb can be nicely explained in terms of orbital interactions between the EH fragments in the $X^2\Pi$ ground state. It would be helpful if the qualitative interpretation of the bonding situation could be supported by a quantitative estimate of the strength of the bonding orbital components that are introduced in the orbital interaction model. This is possible with the help of the energy decomposition analysis (EDA), which is described in the Method section. The EDA gives not only the strength of the intramolecular orbital interactions between the EH fragments but also an estimate of the quasi-classical electrostatic attraction in E_2H_2. We previously employed the EDA for systematically analyzing the nature of the interactions in donor−acceptor bonds[35] and in electron-sharing bonds.[36] Two recent reviews summarize our work in the past.[37]

Table 2 gives the EDA results for structures **A**, **B**, **D1**, and **D2** using two EH molecules in the $X^2\Pi$ ground state as interacting fragments. For the EDA calculations of structure **E** we used the $a^4\Sigma^-$ excited state of EH. The $X^2\Pi \rightarrow a^4\Sigma^-$ excitation energy is then considered as preparation energy of the fragments, which is the reason that the calculated values for ΔE_{prep} of the linear species **E** are rather large.

The EDA data directly lead to an estimate of the bonding contributions of the σ and π orbital components in acetylene and in the calculated heavier homologues of the linear form **E**. Table 2 shows that the overall orbital interaction term ΔE_{orb} contributes between 73.8% (E = Si) and 62.2% (E = Sn) of the attractive interactions. The σ/π ratio of the ΔE_{orb} term remains nearly constant for the elements E. The relative strength of the π bonding is between 41.6% and 44.4% of ΔE_{orb}. We want to point out that the absolute values of the ΔE_{orb} term

(34) At the BP86/QZ4P level, the planar transition state with two bridging hydrogen atoms is calculated to be lower in energy than **D1** by 11.3 kcal/mol for E = Si, 8.8 kcal/mol for E = Ge, 5.4 kcal/mol for E = Sn, and 4.4 kcal/mol for E = Pb.

give only the attractive interactions between electrons that have opposite spin. The orbital interactions between electrons having the same spin is given by the ΔE_{Pauli} term.

Table 3 gives the number of the bonding orbital components as given by the qualitative orbital analysis in the previous section. The numbers in parentheses give the strength of the components, which are estimated by the EDA. The values for **E** come from the σ and π contributions given in Table 2. The data for the σ bond in structure **D2**, which are listed in Table 3, are also directly available from the EDA because the σ bond is the only bonding orbital contribution in this isomer. Note that **E** has a significantly stronger σ bond than **D2**. This is reasonable because the σ bond in **D2** comes formally from a p AO of atom E, while the σ bond in **E** comes formally from a sp hybrid orbital (Figures 2 and 3c). The strength of the orbital components in **D1** can also be directly taken from the EDA results, which give the π-bonding component as the A″ orbital term and the two lone-pair donor−acceptor interactions as the A′ orbital term.

The strength of the orbital components in **A** and **B** cannot directly be taken from the EDA results because of lack of symmetry.[38] The EDA gives only the total orbital interaction in **A**, which according to the orbital analysis has a σ component and a degenerate EH donor−acceptor bond (Figure 3b). The strength of the σ bonding in **A** was estimated by calculating structure **D2**, which has only a σ bond with the E−E bond length of structure **A**. The EDA data of the latter structure are given in Table S1 in the Supporting Information. The difference between the estimated σ-bonding contribution taken from calculating **D2** with the E−E distance of **A** and the total ΔE_{orb} value of **A** gives then the strength of the two EH donor−acceptor bonds. The EDA calculations suggest (Table 3) that an EH donor−acceptor bond is weaker than an E−E σ bond but stronger than a π bond.

Table 2. Energy Decomposition Analysis of E_2H_2 Using the Fragments EH in Their ($X^2\Pi$) Doublet [for **E** ($a^4\Sigma^-$) Quartet State] State (energy values in kcal/mol)

term	A	B	D1	D2	E
			C_2H_2		
ΔE_{int}[e]					−280.0
ΔE_{Pauli}					255.4
ΔE_{elstat}[a]					−147.5 (27.4%)
ΔE_{orb}[a]					−387.9 (72.6%)
$\Delta E(\text{A}')$[b]					−215.5 (55.6%)
$\Delta E(\text{A}'')$[b]					−172.4[d] (44.4%)
ΔE_{prep}					40.0
$\Delta E\ (=-D_e)$					−240.0
			Si_2H_2		
ΔE_{int}	−92.5	−81.4	−67.2	−42.1	−125.0
ΔE_{Pauli}	286.9	229.6	162.1	101.4	109.9
ΔE_{elstat}[a]	−128.9 (34.0%)	−118.2 (38.0%)	−82.3 (35.9%)	−68.6 (47.8%)	−61.5 (26.2%)
ΔE_{orb}[a]	−250.2 (66.0%)	−192.9 (62.0%)	−147.0 (64.1%)	−74.9 (52.2%)	−173.4 (73.8%)
$\Delta E(\text{A}')$[b]	−250.2[c] (100.0%)	−149.1 (77.3%)	−105.3 (71.6%)	−74.9 (>99.9%)	−96.9 (55.9%)
$\Delta E(\text{A}'')$[b]		−43.7 (22.7%)	−41.7 (28.3%)	<−0.1 (<0.1%)	−76.5[d] (44.1%)
ΔE_{prep}	6.5	5.3	1.2	1.8	80.5
$\Delta E\ (=-D_e)$	−86.0	−76.1	−66.0	−40.3	−44.5
			Ge_2H_2		
ΔE_{int}	−82.0	−69.7	−54.6	−38.6	−118.6
ΔE_{Pauli}	268.9	217.9	146.3	92.2	135.9
ΔE_{elstat}[a]	−137.5 (39.2%)	−127.8 (44.5%)	−82.5 (41.1%)	−67.8 (51.8%)	−85.5 (33.6%)
ΔE_{orb}[a]	−213.3 (60.8%)	−159.8 (55.5%)	−118.4 (58.9%)	−63.0 (48.2%)	−169.0 (66.4%)
$\Delta E(\text{A}')$[b]	−213.3[c] (100.0%)	−122.0 (76.3%)	−81.7 (69.0%)	−62.9 (99.8%)	−96.4 (57.0%)
$\Delta E(\text{A}'')$[b]		−37.8 (23.7%)	−36.7 (31.0%)	−0.1 (0.2%)	−72.6[d] (43.0%)
ΔE_{prep}	7.2	5.9	1.8	1.4	99.6
$\Delta E\ (=-D_e)$	−74.8	−63.8	−52.4	−37.2	−19.0
			Sn_2H_2		
ΔE_{int}	−69.4	−54.5	−40.1	−34.4	−95.5
ΔE_{Pauli}	224.2	174.9	113.6	81.1	115.0
ΔE_{elstat}[a]	−127.1 (43.3%)	−111.9 (48.8%)	−68.7 (44.7%)	−63.8 (55.3%)	−79.5 (38.0%)
ΔE_{orb}[a]	−166.5 (56.7%)	−117.5 (51.2%)	−85.0 (55.3%)	−51.6 (44.7%)	−131.0 (62.2%)
$\Delta E(\text{A}')$[b]	−166.5[c] (100.0%)	−89.0 (75.7%)	−57.5 (67.6%)	−51.5 (99.8%)	−76.6 (58.5%)
$\Delta E(\text{A}'')$[b]		−28.6 (24.3%)	−27.6 (34.4%)	−0.1 (0.2%)	−54.5[d] (41.6%)
ΔE_{prep}	7.1	5.7	3.1	1.4	97.8
$\Delta E\ (=-D_e)$	−62.3	−48.8	−37.0	−33.0	2.3
			Pb_2H_2		
ΔE_{int}	−64.3	−44.2	−27.8	−32.0	−81.1
ΔE_{Pauli}	209.1	138.1	77.4	74.8	117.7
ΔE_{elstat}[a]	−129.0 (47.2%)	−94.1 (51.6%)	−45.7 (43.5%)	−61.8 (57.9%)	−73.6 (37.0%)
ΔE_{orb}[a]	−144.5 (52.8%)	−88.1 (48.4%)	−59.5 (56.5%)	−45.0 (42.1%)	−125.2 (63.0%)
$\Delta E(\text{A}')$[b]	−144.5[c] (100.0%)	−63.9 (72.5%)	−36.2 (60.9%)	−44.[g] (99.8%)	−71.9 (57.4%)
$\Delta E(\text{A}'')$[b]		−24.3 (27.5%)	−23.2 (39.1%)	−0.1 (0.2%)	−53.3[d] (42.6%)
ΔE_{prep}	6.8	3.8	1.3	1.0	116.1
$\Delta E\ (=-D_e)$	−57.5	−40.4	−26.5	−31.0	35.0

[a] The value in parentheses gives the percentage contribution to the total attractive interactions $\Delta E_{\text{elstat}} + \Delta E_{\text{orb}}$. [b] The value in parentheses gives the percentage contribution to the total orbital interactions ΔE_{orb}. [c] The symmetry of structure **A** in the analysis is C_1. [d] The value gives the total contribution of the π orbitals to the ΔE_{orb} term. The symmetry of structure **E** in the analysis is $C_{\infty v}$ [e] Structures **A**, **B**, **D1**, and **D2** of C_2H_2 are not stationary points on the singlet ground-state PES.

(35) (a) Diefenbach, A.; Bickelhaupt, F. M.; Frenking, G. *J. Am. Chem. Soc.* **2000**, *122*, 6449. (b) Uddin, J.; Frenking, G. *J. Am. Chem. Soc.* **2001**, *123*, 1683. (c) Lein, M.; Frunzke, J.; Timoshkin, A.; Frenking, G. *Chem. Eur. J.* **2001**, *7*, 4155. (d) Frenking, G.; Wichmann, K.; Fröhlich, N.; Grobe, J.; Golla, W.; Le Van, D.; Krebs, B.; Läge, M. *Organometallics* **2002**, *21*, 2921. (e) Frunzke, J.; Lein, M.; Frenking, G. *Organometallics* **2002**, *21*, 3351. (f) Cases, M.; Frenking, G.; Duran, M.; Solà, M. *Organometallics* **2002**, *21*, 4182. (g) Rayón, V. M.; Frenking, G. *Chem. Eur. J.* **2002**, *8*, 4693. (h) Nemcsok, D. S.; Kovács, A.; Rayón, V. M.; Frenking, G. *Organometallics* **2002**, *21*, 5803. (i) Dörr, M.; Frenking, G. *Z. Allg. Anorg. Chem.* **2002**, *628*, 843. (j) Loschen, C.; Voigt, K.; Frunzke, J.; Diefenbach, A.; Diedenhofen, M.; Frenking, G. *Z. Allg. Anorg. Chem.* **2002**, *628*, 1294. (k) Pandey, K. K.; Lein, M.; Frenking, G. *J. Am. Chem. Soc.* **2003**, *125*, 1660. (l) Lein, M.; Frunzke, J.; Frenking, G. *Angew. Chem.* **2003**, *115*, 1341; *Angew. Chem., Int. Ed.* **2003**, *42*, 1303. (m) Lein, M.; Frunzke, J.; Frenking, G. *Inorg. Chem.* **2003**, *42*, 2504. (n) Massera, C.; Frenking, G. *Organometallics* **2003**, *22*, 2758. (o) Rayón, V. M.; Frenking, G. *Organometallics* **2003**, *22*, 3304. (p) Esterhuysen, C.; Frenking, G. *Chem. Eur. J.* **2003**, *9*, 3518. (q) Dietz, O.; Rayón, V. M.; Frenking, G. *Inorg. Chem.* **2003**, *42*, 4977. (r) Lein, M.; Szabó, A.; Kovács, A.; Frenking, G. *Faraday Discuss.* **2003**, *124*, 365. (s) Esterhuysen, C.; Frenking, G. *Chem. Eur. J.* **2003**, *9*, 3518. (t) Bessac, F.; Frenking, G. *Inorg. Chem.* **2003**, *42*, 7990. (u) Loschen, C.; Frenking, G. *Inorg. Chem.* **2004**, *43*, 778. (v) Nechaev, M. S.; Rayón, V. M.; Frenking, G *J. Phys. Chem. A* **2004**, *108*, 3134. (w) Pandey, K. K.; Lein, M.; Frenking, G. *Organometallics* **2004**, *23*, 2944. (x) Petz, W.; Kutschera, C.; Heitbaum, M.; Frenking, G.; Tonner, R.; Neumüller, B. *Inorg. Chem.* **2005**, *44*, 1263.

(36) (a) Esterhuysen, C.; Frenking, G. *Theor. Chem. Acc.* **2004**, *111*, 381. (b) Kovács, A.; Esterhuysen, C.; Frenking, G. *Chem. Eur. J.* **2005**, *11*, 1813. (c) Cappel, D.; Tüllmann, S.; Krapp, A.; Frenking, G. *Angew. Chem.*, in press.

(37) (a) Frenking, G.; Wichmann, K.; Fröhlich, N.; Loschen, C.; Lein, M.; Frunzke, J.; Rayón, V. M. *Coord. Chem. Rev.* **2003**, *238*−*239*, 55. (b) Lein, M.; Frenking, G. *Theory and Applications of Computational Chemistry: The First 40 Years*; Dykstra, C. E., Kim, K. S., Frenking, G., Scuseria, G. E., Eds.; Elsevier: Amsterdam, in press.

(38) Note that the symmetry in the EDA calculations is not given by the overall symmetry of the molecule but by the symmetry of the fragments with respect to the entire molecule. Thus, the EDA of structure **A** has only C_1 symmetry because the EH fragments are in neither of the two mirror planes of the E_2H_2 geometry.

Table 3. Number and EDA Values (given in parentheses in kcal/mol) of the Stabilizing Orbital Interactions in E_2H_2 Structures **A, B, D1, D2,** and **E**

bonding type	A	B	D1	D2	E
			C_2H_2		
σ bond					1 (215.5)
π bond					2 (2 × 86.2)
EH-donation					
Lp-donation					
Σ					3 (387.9)
			Si_2H_2		
σ bond	1 (116.8)			1 (74.9)	1 (96.9)
π bond		1 (43.7)	1 (41.7)		2 (2 × 38.25)
EH-donation	2 (2 × 66.7)	1 (77.5)			
Lp-donation		1 (71.7)	2 (2 × 52.65)		
Σ	3 (250.2)	3 (192.9)	3 (147.0)	1 (74.9)	3 (173.4)
			Ge_2H_2		
σ bond	1 (94.5)			1 (62.9)	1 (96.4)
π bond		1 (37.8)	1 (36.7)		2 (2 × 36.3)
EH-donation	2 (2 × 59.4)	1 (70.2)			
Lp-donation		1 (51.8)	2 (2 × 40.85)		
Σ	3 (213.3)	3 (159.8)	3 (118.4)	1 (62.9)	3 (169.0)
			Sn_2H_2		
σ bond	1 (71.1)			1 (51.5)	1 (76.6)
π bond		1 (28.6)	1 (27.6)		2 (2 × 27.25)
EH-donation	2 (2 × 47.7)	1 (54.8)			
Lp-donation		1 (34.1)	2 (2 × 28.75)		
Σ	3 (166.5)	3 (117.5)	3 (85.0)	1 (51.5)	3 (131.0)
			Pb_2H_2		
σ bond	1 (59.9)			1 (44.8)	1 (71.9)
π bond		1 (24.3)	1 (23.2)		2 (2 × 26.65)
EH-donation	2 (2 × 42.3)	1 (43.6)			
Lp-donation		1 (20.2)	2 (2 × 18.15)		
Σ	3 (144.5)	3 (88.1)	3 (59.5)	1 (44.8)	3 (125.2)

The strength of the orbital components in **B**, which has a π bond and one EH and one lone-pair donor−acceptor bond (Figure 4a), was estimated in a similar way as for **A**. The π-bonding component in **B** is directly available from the EDA calculations because the overall symmetry of the fragments in the molecule is C_s.[38] Thus, the calculated data for $\Delta E(A'')$ give the strength of the π bond. The lp donor−acceptor component was taken from EDA calculations of structure **D1**, where the E−H and E−H distances and the E−E−H bond angle were held fixed at the values of **B**. The EDA data of the latter structure are given as Table S2 in the Supporting Information. The difference between the total ΔE_{orb} value of **B** and the two components, i.e., π bond and lp donor−acceptor bond, gives an estimate of the EH donor−acceptor bond strength. Table 3 shows that the lp donor−acceptor bond in **B** is stronger than in **D1** and that the EH donor−acceptor bond is stronger than in **A**. The strength of the E−E σ bond shows the trend **B** > **D1** > **E**, but the differences are not very large.

5. Singlet and Triplet Structures of Si_2H_2

Two questions about the PES of E_2H_2 are still open that need to be addressed. One question concerns the accuracy of the calculated relative energies of the isomers at BP86/QZ4P compared with high-level ab initio data. The second question concerns the possibility that energetically low-lying isomeric forms of E_2H_2 may exist on the triplet PES. We searched for equilibrium structures of Si_2H_2 in the triplet state by geometry optimizations at BP86/QZ4P using numerous starting geometries with different orbital occupations. We think that the heavier E_2H_2 triplet species with E = Ge−Pb which have not been investigated by us should have structures similar to those of Si_2H_2. The energies of the singlet and triplet structures optimized at BP86/QZ4P were then calculated at the MRCI-SD/aug-cc-pVQZ level. A full-valence (10/10)CAS/aug-cc-pVQZ wave function was used as reference. The results are shown in Figure 6.

The calculated relative energies of the singlet species at MRCI-SD/aug-cc-pVQZ agree very well with the BP86/QZ4P data. The ab initio values are systematically smaller than the DFT results. The largest deviation is calculated for structure **D2**, where the difference between the ab initio value and the DFT result is 5.3 kcal/mol. Triplet structures of Si_2H_2 which are similar to the singlet isomers **A**, **B**, and **C** have been located as minima on the PES, but the energy ordering of the triplet species **A(T)**−**C(T)** is different from the singlet states. The doubly bridged isomer **A(T)** is the highest lying energy minimum that was found on the singlet and triplet PES. Note that the relative energies of the triplet species that are predicted at MRCI-SD/aug-cc-pVQZ are now always *larger* than the BP86/QZ4P data. The deviation is up to 13.8 kcal/mol for **G(T)**, which is a transition state. An approximate estimate of the higher excitation in the MRCI-SD calculations using the Davidson correction[39] does not lead to significant changes. Table S3 of the Supporting Information gives the total and relative energies at MRCI-SD/aug-cc-pVQZ and at MRCI-SD(Q)/aug-cc-pVQZ, where the (Q) indicates the inclusion of the Davidson correction. The relative energies of the isomers of Si_2H_2 show differences of <2 kcal/mol between the two levels of theory, except for **A(T)** and **G(T)**, where slightly larger deviations of ∼4 kcal/mol are found. The relative energies of the latter species

(39) Langhoff, S. R.; Davidson, E. R. *Int. J. Quantum Chem.* **1974**, *8*, 61.

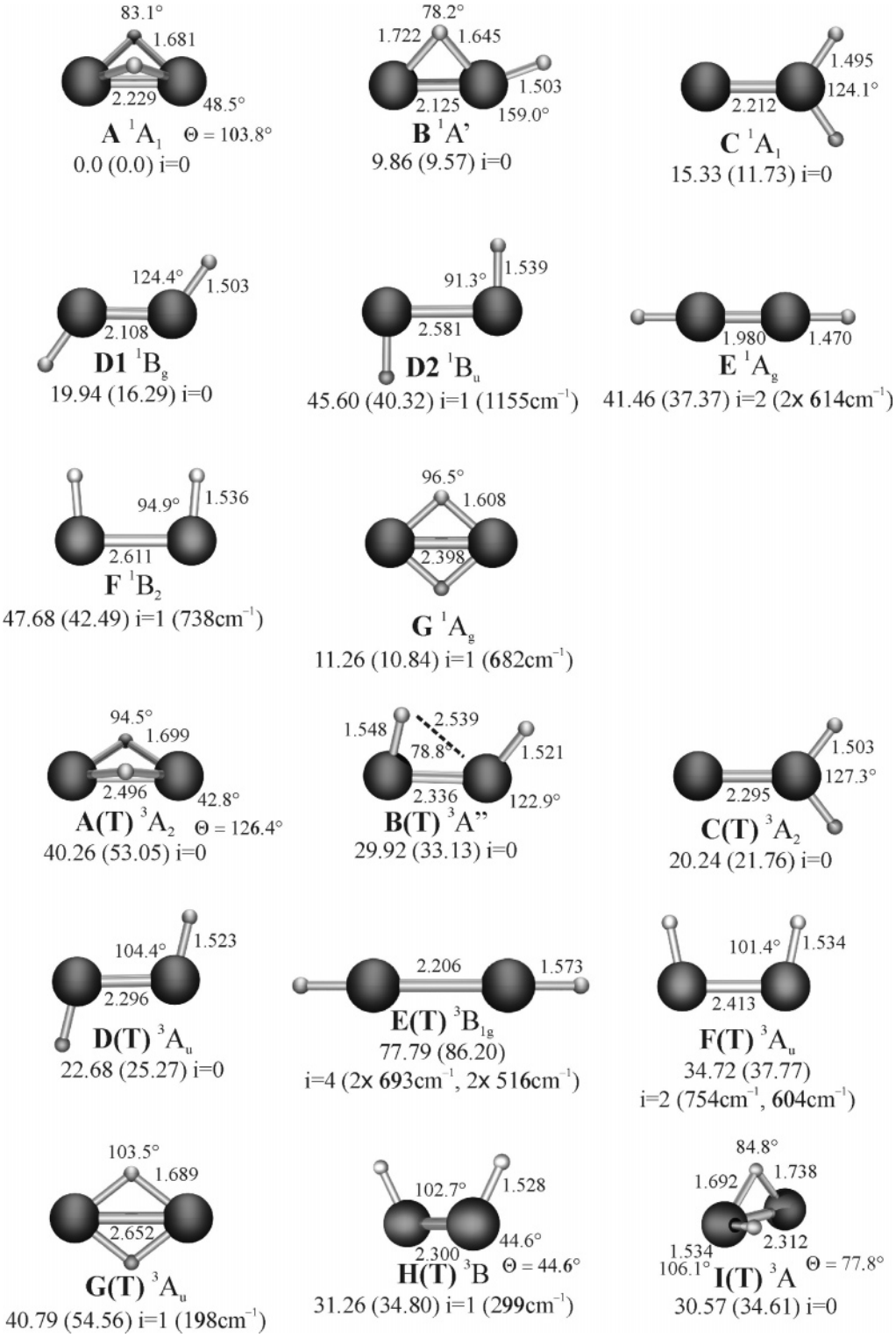

Figure 6. Calculated equilibrium structures of Si_2H_2 on the singlet and triplet PES at BP86/QZ4P. Bond lengths are given in Å, angles in deg. The values of Θ for structures **A**, **A(T)**, **H(T)**, and **I(T)** give the dihedral angle between the Si_2H and Si_2H' planes. The relative energies with respect to **A** at BP86/QZ4P (MRCI-SD/aug-cc-pVQZ//BP86/QZ4P values in parentheses) are given at the bottom of each entry in kcal/mol together with the number and absolute values of the imaginary frequencies.

with respect to **A** at MRCI-SD(Q)/aug-cc-pVQZ are 49.06 kcal/mol for **A(T)** and 50.14 kcal/mol for **G(T)**, which deviate less from the BP86/QZ4P data than the MRCI-SD/aug-cc-pVQZ values.

We found only one equilibrium structure **D(T)** which has a planar trans-bent arrangement of the SiH fragments. The energy minimum **D(T)** is not much higher in energy than the singlet form **D1** (Figure 6). The linear form **E(T)**, which is a fourth-order saddle point (i = 4), is even much higher in energy than **E**. Structure **F(T)** is energetically lower lying than singlet **F**, but the former species has two imaginary frequencies while the latter has only one. Two relatively low-lying geometrical forms have been optimized on the triplet PES which we did not find on the singlet PES. The C_2 symmetric species **H(T)** is a

transition state but the nonplanar singly bridged isomer **I(T)** is an energy minimum on the PES.

6. Summary

The unusual equilibrium structures of the heavy-atom group 14 analogues of acetylene E_2H_2 with E = Si, Ge, Sn, and Pb can be explained with the interactions between the EH moieties in the ($X^2\Pi$) electronic ground state which differ from C_2H_2, which is bound through interactions between CH in the $a^4\Sigma^-$ excited state. Bonding between two ($X^2\Pi$) fragments of the heavier EH hydrides is favored over the bonding in the $a^4\Sigma^-$ excited state, leading to triply bonded linear species HE≡EH because the $X^2\Pi \rightarrow a^4\Sigma^-$ excitation energy of EH (E = Si, Ge, Sn, Pb) is significantly higher than for CH, while the stabilizing contribution of the π bonds becomes less. The doubly bridged global energy minimum **A** of E_2H_2 has three bonding orbital contributions: one σ bond and two donor−acceptor bonds of the E−H bonding orbitals. The singly bridged isomer **B** also has three bonding orbital contributions: one π bond, one E−H donor−acceptor bond, and one lone-pair donor−acceptor bond. The trans-bent form **D1** has one π bond and two lone-pair donor−acceptor bonds, while **D2** has only one σ bond as stabilizing orbital contribution. The strength of the stabilizing orbital contributions in the different isomers of E_2H_2 has been estimated with an energy decomposition analysis, which gives also the bonding contributions of the quasi-classical electrostatic interactions. MRCI calculations of stationary points of Si_2H_2 on the singlet and triplet PES show that the triplet species are higher in energy than the singlet structures. The calculated relative energies at the BP86 and MRCI level of theory agree quite well with each other.

Acknowledgment. This work was supported by the Deutsche Forschungsgemeinschaft. Excellent service by the Hochschulrechenzentrum of the Philipps-Universität Marburg is gratefully acknowledged. Additional computer time was provided by the HLRS Stuttgart and the HHLR Darmstadt.

Supporting Information Available: Tables S1 and S2, with the EDA results of **D1** and **D2** calculated under geometry constraints as described in the text. Table S3, with the total and relative energies of the Si_2H_2 forms **A**−**I(T)**. Table S4, with the absolute energies of the DFT calculations. Complete refs 24 and 29. This material is available free of charge via the Internet at http://pubs.acs.org.

JA042295C